

## Multi-scale simulation of droplet-droplet interactions and coalescence

<sup>1,2</sup>Ndivhuwo M. Musehane\*, <sup>1</sup>Oliver F. Oxtoby and <sup>2</sup>Daya B. Reddy

1. Aeronautic Systems, Council for Scientific and Industrial Research, P.O Box 395, Pretoria, 0001, South Africa.
2. University of Cape Town, Department of Mathematics and Applied Mathematics and Centre for Research in Computational and Applied Mechanics, Rondebosch, 7701, South Africa.

\* nmusehane@csir.co.za

### ABSTRACT

In this work, droplet-droplet interaction is modelled using a multiphase flow computational fluid dynamics approach coupled with a reduced order surface thin-film model. An existing multiphase flow model based on a multiple marker volume of fluid method is extended to include the thin-film model that is derived to simulate film drainage on the sub-grid scale. This allows for the prediction of coalescence or rebound of colliding droplets from first principles. The model is implemented into the open source tool set OpenFOAM<sup>®</sup> and tested against experimental results of colliding hydrocarbon droplets in the literature. It is found to produce accurate interface deformation results for the duration of the collision, and to consistently predict the outcome of the collision.

### KEYWORDS

Coalescence, Droplets, VOF, Film drainage

### INTRODUCTION

This work consists of the development, numerical implementation and validation of a reduced order surface thin film model coupled to the multiple marker volume of fluid (VOF) method [1, 2], to model droplet-droplet interactions and the resultant coalescence or rebound. Droplet-droplet interactions are found in various industrial processes and their coalescence influences the hydrodynamic and fluid transport phenomena that govern the overall flow behaviour. It is found to affect the droplet size distribution and shape which influence the overall optimal operating conditions. However, there are difficulties in modelling the collision process computationally.

The various multiphase flow modelling techniques available differ in their description and treatment of the droplet-fluid interface. Euler-Euler and Euler-Lagrange type methods lack in that they rely heavily on prior knowledge of the flow structure in the form of empirical correlations when modelling coalescence [3]. On the other hand, interface tracking methods [4] can be computationally intensive due to the mesh deformations required and, due to mesh entanglement, struggle to capture large topology changes that result when droplets interact. This work endeavours to eliminate the need to use empirical correlations based on phenomenological models by developing a multi-scale model that predicts the outcome of a collision between droplets from first principles but at a reduced computational cost.

The equations that govern incompressible immiscible droplets dispersed in a continuous fluid phase undergoing isothermal and laminar Newtonian three-dimensional flow are the volume averaged conservation of mass, momentum, and liquid-gas interface advection equations,

$$\nabla \cdot (\rho \mathbf{u}) = 0, \quad (1)$$

$$\frac{\partial(\rho \mathbf{u})}{\partial t} + \nabla \cdot (\rho \mathbf{u} \mathbf{u}) = -\nabla p + \nabla \cdot (\mu \nabla \mathbf{u}) + \rho \mathbf{g} + \sum_{\theta=1}^N \sigma \kappa_{\theta}^s \nabla \alpha_{\theta} \text{ and} \quad (2)$$

$$\frac{\partial \alpha_{\theta}}{\partial t} + \nabla \cdot (\alpha_{\theta} \mathbf{u}) = 0 \quad (3)$$

where

$$\kappa_{\theta}^s = \frac{\nabla \alpha_{\theta}^s}{|\nabla \alpha_{\theta}^s|}, \quad (4)$$

$$\alpha_{\theta}^s - \alpha_{\theta} = \nabla^2 (\eta \alpha_{\theta}^s). \quad (5)$$

Here  $\rho$  is the density,  $\mathbf{u}$  is the velocity,  $p$  is the pressure,  $\mu$  is the dynamic viscosity,  $\mathbf{g}$  is the gravitational acceleration,  $N$  gives the number of droplets,  $\sigma$  is the surface tension coefficient, and  $\alpha_{\theta}$  is the volume fraction field assigned different values for multiple droplets containing the same fluid.

The last term on the RHS of equation (2) is the surface tension force obtained from the Continuum Surface Force (CSF) formulation [5] where  $\kappa_{\theta}^s$  is the signed curvature calculated from smoothed volume fraction field values  $\alpha_{\theta}^s$  to improve the numerical calculation of second order gradients [6].

The formulation above is known as the multiple marker VOF method, which uses separate indicator functions  $\alpha_{\theta}$  for each droplet and is essential to prevent premature numerical coalescence. Although simple and straightforward to implement computationally, as it stands it lacks in that it prevents coalescence in all circumstances [2]. Thus, to model coalescence with this model this work extends the method to include a reduced order surface thin film model that will correctly predict the outcome of droplet-droplet collisions. Once coalescence is detected, the separate indicator functions are merged.

### COALESCENCE MODEL

The collision process between droplets can be described in three stages based on the film drainage theory of coalescence [7]. Consider two droplets; Stage 1 is when they approach each other, and as they do so a thin film of the surrounding fluid is trapped between them; Stage 2 is when this fluid film drains out; and lastly in Stage 3 the droplets will either coalesce if the thin film attains a critical thickness  $h_{Crit}$ , becomes unstable and ruptures; or bounce apart if the fluid film does not attain  $h_{Crit}$ .

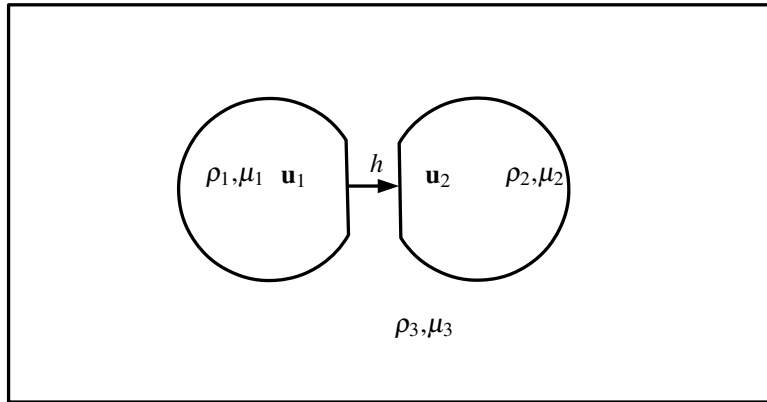


Figure 1: Two droplets with radius  $R$  approaching each other with velocities  $\mathbf{u}_1$  and  $\mathbf{u}_2$  forming a locally planar thin film

The thin film thus is an important aspect in modelling coalescence. The method developed here is aimed at modelling the dynamics of the thin liquid film during Stage 2 and Stage 3 of the collision process. It calculates the thickness of the thin film and compares it to a critical film thickness to decide whether coalescence should occur. Due to the extremely small scale of the thin film (typically  $h_{Crit}$  is of the order of micrometres) a multiscale model is essential, where calculation of the film thickness occurs on the sub-grid scale.

The sub-grid model is based on the Reynolds equation for two moving interfaces from lubrication theory [8]. It is derived based on the following assumptions: the thin film thickness  $h$  is assumed to be much

smaller than the radius  $R$  of the droplets ( $h \ll R$ ). This implies that the region between the interfaces of the two droplets can be assumed to be locally planar (1) with the thin film locally resembling either a box in three dimensions or a tube in two dimensions. In this region, the effects of gravity and surface tension are negligible. The pressure gradient across the thickness of the thin film is assumed to be constant. With these assumptions it can be shown that the momentum equations can be reduced to

$$\frac{\partial(\rho h)}{\partial t} + \mathbf{Q} \cdot [\nabla \rho h - (\nabla \rho h \cdot \mathbf{n})\mathbf{n}] = \nabla \cdot \left[ \frac{-\rho h^3}{12\mu} [\nabla p - (\nabla p \cdot \mathbf{n})\mathbf{n}] \right], \quad (6)$$

where  $\mathbf{n}$  is defined as a unit vector normal to the interface and

$$\mathbf{Q} = \frac{\mathbf{u}_1 + \mathbf{u}_2}{2}, \quad (7)$$

is the interface velocity vector.

## NUMERICAL IMPLEMENTATION

The model equations are made up of equations (1)–(7). Equations (1)–(4) govern the flow between colliding droplets while equations (6)–(7) determine the outcome of the collision by evaluating the thickness of the thin liquid film.

A Finite Volume Method (FVM) of discretization is followed, where the integral form of the governing equations on a finite number of non-overlapping control volumes is used to obtain a system of coupled nonlinear equations.

The solution to equation (6) gives the thickness  $h$  of the thin film between two interfaces. In this study, the pressure obtained from the solution of the Navier-Stokes equation is used together with an initial film thickness estimate  $h_{Est}$  to obtain a new value of the film thickness. Equation (6) is only valid when the droplets are close to each other.

The pressure used in equation (6) is obtained from the flow simulation since it is primarily determined by the dynamics on the grid scale, i.e. by the impulse acting to decelerate the colliding droplets. An alternative approach is taken by Mason *et al.* [9], where the rate of change of film thickness is obtained from the velocity field of the flow solution, and the pressure is solved for in the film equation (in keeping with traditional applications of the Reynolds equation). This approach has been avoided since the film-thinning velocity is extremely small and difficult to detect compared to the larger flow velocities superimposed on it. Indeed, the rate of film-thinning is not reliably calculated by the flow equations as it stems from the film-drainage mass balance in the sub-grid region.

The solution procedure thus involves firstly devising a way to measure the initial separation distance  $h_{Est}$  between the droplets that is valid for separation of a few mesh cells or greater. A graphical approach based on measuring the distance from each volume fraction is used to obtain the separation  $h_{Est}$  between the particles.

Consider two interfaces that enclose fluids described by the volume fraction fields  $\alpha_1$  and  $\alpha_2$  which are close to each other in a computational domain. Consider lines which start from the interfaces pointing in the direction of the outward unit normal to the interface  $\mathbf{n}_1^s$  and  $\mathbf{n}_2^s$  given by

$$\mathbf{n}_1^s = \frac{\nabla(\alpha_1^s)}{|\nabla(\alpha_1^s)|}, \quad \mathbf{n}_2^s = \frac{\nabla(\alpha_2^s)}{|\nabla(\alpha_2^s)|}. \quad (8)$$

Define the length from a point on the interface  $\mathbf{x}_i$  to a point  $\mathbf{x}$  on a ray by the path integral along the ray in the unit normal directions,

$$h_{Est1} = \int_{\mathbf{x}_i}^{\mathbf{x}} (1 - \alpha_1) \mathbf{n}_1^s \cdot d\mathbf{l}, \quad (9)$$

and

$$h_{Est2} = \int_{\mathbf{x}_i}^{\mathbf{x}} (1 - \alpha_2) \mathbf{n}_2^s \cdot d\mathbf{l}. \quad (10)$$

The path integrals (9) and (10) start from the interface so a switch is used to set the initial value at the interface to zero. To achieve this, the above two equations need to be nullified and replaced with  $h_{Est_1} = 0$  and  $h_{Est_2} = 0$  inside the droplet, so we multiply both sides of equations (9) and (10) by boolean switches  $[1 - \text{pos}(\alpha_1 - 0.95)]$  and  $[1 - \text{pos}(\alpha_2 - 0.95)]$  respectively, and add  $\text{pos}(\alpha_1 - 0.95)h_{Est_1}$  and  $\text{pos}(\alpha_2 - 0.95)h_{Est_2}$  to the respective equations so that when  $\alpha_1 > 0.95$  and  $\alpha_2 > 0.95$  we end up with  $h_{Est_1} = 0$  and  $h_{Est_2} = 0$ . Here the function  $\text{pos}(s)$  is a positive boolean given by

$$\text{pos}(s) = \begin{cases} 1 & s \geq 0, \\ 0 & s < 0. \end{cases} \quad (11)$$

Rewriting equations (9) and (10) in differential form, also considering the above arguments, the equations for  $h_{Est_1}$  and  $h_{Est_2}$  become

$$[1 - \text{pos}(\alpha_1 - 0.95)](\nabla h_{Est_1} \cdot \mathbf{n}_1^s) = [1 - \text{pos}(\alpha_1 - 0.95)](1 - \alpha_1) + \text{pos}(\alpha_1 - 0.95)h_{Est_1} \quad (12)$$

and

$$[1 - \text{pos}(\alpha_2 - 0.95)](\nabla h_{Est_2} \cdot \mathbf{n}_2^s) = [1 - \text{pos}(\alpha_2 - 0.95)](1 - \alpha_2) + \text{pos}(\alpha_2 - 0.95)h_{Est_2}. \quad (13)$$

In the region between the two interfaces, the sum of  $h_{Est_1}$  and  $h_{Est_2}$  gives the separation distance between the interfaces. Thus the estimate  $h_{Est}$  is obtained from

$$h_{Est} = h_{Est_1} + h_{Est_2} \quad (14)$$

since this gives the sum of the distance to interface 1 along the ray in direction  $\mathbf{n}_1^s$  and the distance to interface 2 along the ray in direction  $\mathbf{n}_2^s$  from any given point. This approach cannot however be used to obtain distances that are smaller than a mesh cell spacing. The value of  $h_{Est}$  is used as an initial condition for the Reynolds equation.

From this initial separation distance, a region in space can be calculated that determines where the Reynolds equation is valid. For this purpose we define a switch  $\beta$  that turns the computation of the Reynolds equation on when the separation estimate  $h_{Est}$  spans a few mesh cells and turns it off for larger separations. A multiple of the mesh spacing estimate is used to restrict and the mesh cells in which equation (6) is actually calculated. This restricts the calculation of the equation to areas that are very close to the thin film region. The boolean switch which identifies the region is defined by

$$\beta = \text{pos}(\xi \delta h - h_{Est}) \text{pos}(\alpha_1^s - 0.001) \text{pos}(\alpha_2^s - 0.001) \quad (15)$$

where  $\xi$  is a parameter that determines the width of the region where the thin film equation is solved as a multiple of the mesh spacing  $\delta h$ .

There is a numerical discontinuity between the values of  $h$  inside the thin film region  $\beta$  and those outside that have been pegged to  $h_{Est}$ . Evaluation of the gradient of  $h$  would be incorrect for computational cells that surround the thin film region. To avoid the discontinuity of the gradient of  $h$  at the boundary of the thin film region the gradient of  $h$  is evaluated in a reduced thin film region  $\beta^*$  which excludes the outermost layer of cells in the region defined by  $\beta$ .

The discretized form of equation (6) evaluated using an implicit Euler scheme is given by

$$\beta \frac{\rho_P h_P^{m+1} - \rho_P h_P^m}{\Delta t} V_P + \beta \mathbf{Q} \cdot [\nabla \rho_P h_P^{m+1} - (\nabla \rho_P h_P^{m+1} \cdot \mathbf{n}) \mathbf{n}] V_P + (1 - \beta) h_P^{m+1} V_P = \beta \frac{-\rho_f (h_f^{m+1})^3}{12\mu_f} \sum_f \mathbf{A}_f \cdot (\nabla p_t^s)_f^{m+1} + \beta^* \frac{-3\rho_f (\overline{\nabla p_t^s})_f^{m+1} (h_f^{m+1})^2}{12\mu_f} \mathbf{A}_f h_f^{m+1} + (1 - \beta) h_{Est}^{m+1} V_P, \quad (16)$$

where subscript  $(\cdot)_P$  and  $(\cdot)_f$  are quantities evaluated at the cell centres and cell faces of the control volume while  $(\cdot)^{m+1}$  and  $(\cdot)^m$  are values evaluated at the new and old time step.  $V_P$  is the volume of the computational control volume, and  $\mathbf{A}_f$  is the surface area vector that points in the unit normal direction to the interface.

For simplicity the tangential pressure term has been assigned a new symbol  $\nabla p_t = \nabla p - (\nabla p \cdot \mathbf{n})\mathbf{n}$ . In order to calculate the pressure gradient in the sub-grid region between the droplets, the surface tension pressure jump is removed by subtracting the surface tension force from the tangential pressure as follows:

$$\overline{\nabla p_t^s} = \nabla p_t - \sum_{\theta=1}^N \sigma \kappa_{\theta}^s \nabla \alpha_{\theta}. \quad (17)$$

The solution procedure of the model is as follows:

- Set-up initial and boundary conditions
- Calculate the available fluxes and the multiple VOF fields
- Assemble the momentum equation
- Assemble and solve the pressure equation using a pressure correction algorithm PISO
- Calculate initial  $h_{Est}$
- Where  $h_{Est}$  is within a certain number of mesh cells
  - Solve the reduced order surface thin film equations to obtain  $h$
  - If  $\min(h) < h_{Crit}$ 
    - \* Merge the volume fraction fields
  - Where  $h_{Est}$  is too large
    - \* Set  $h = h_{Est}$
    - \* Do not solve the reduced order surface thin film equations
- Move on to the next time-step and repeat until final time is reached

## NUMERICAL EVALUATION

In this section the implementation of the reduced order surface thin film model coupled to the multiple marker VOF method is tested against the experiment of [10]. The experiment provides detailed time resolved interface deformation images of the head on collision of two identical Tetradecane ( $C_{14}H_{30}$ ) droplets in 1 atm Nitrogen gas. The material properties are shown in Table 1.

	Liquid (Tetradecane)	Gas (Nitrogen)
Density ( $\text{kgm}^{-3}$ )	762	1.225
Viscosity ( $\mu\text{m}$ )	107.2	170.6
Surface Tension ( $\text{kgs}^{-2}$ )	0.0265	

Table 1: Material Properties for Tetradecane and Nitrogen at 20°C [10]

Quantity	Case I	Case II	Case III	Case IV
$U_0$ ( $\text{ms}^{-1}$ )	0.302	0.24	0.496	0.596
R ( $\mu\text{m}$ )	107.2	170.6	167.6	169.7
$We$	2.25	2.26	9.33	13.63
T (ms)	0.415	0.831	0.811	0.826

Table 2: Physical Quantities [10]

Four test cases were studied: the first two result in droplet coalescence and rebound with minimal droplet deformation while the last two produce the same results with large deformations in the droplet shapes.

The experimental parameters, viz. individual droplet velocity  $U_0$ , droplet radius  $R$  and the Weber number  $We = \frac{2\rho U_0^2 D}{\sigma}$  for each case are shown in Table 2. The experimental results were normalized by the droplet oscillation period  $T = 2\pi \left(\frac{\rho_l R^3}{8\sigma}\right)^{1/2}$  [10] where  $\rho_l$  is the density of Tetradecane.

Since the radii of the droplets is of the order  $O(10^{-6})$ , gravity is negligible compared to surface tension forces and the term  $\rho \mathbf{g}$  in the momentum equation is neglected. The simulations are performed on an axisymmetric structured, Cartesian and uniform mesh. The domain dimensions are  $4D \times 2D$  where  $D$  is the corresponding droplet diameter. The droplets are initialised a distance of  $1.5D$  apart. The boundary conditions for the pressure are set to zero gradient at the walls with an internal air pressure set to 1 atm. A no slip velocity boundary condition is set at the walls with an initial internal gas velocity of zero and velocity within each droplet set to  $U_0$ . The computational domain is shown in figure 2.



Figure 2: Axisymmetric case set-up

The solution procedure as mentioned before involves firstly obtaining the initial thin film thickness estimate to define the thin film region  $\beta$  and secondly determining the critical film thickness  $h_{Crit}$ .

In the determination of the thin film region  $\beta$ , the numerical parameter  $\xi$  is required to determine the mesh cell spacing at which to switch from the geometric determination of the initial separation distance between droplet interfaces  $h_{Est}$  to the solution through the surface thin film model. The restrictions on  $\xi$  are that it should be big enough that the geometric determination spans several mesh cells to make it valid, but it should not be too big (resulting in  $\beta$  spanning too many mesh cells) because the surface thin film model is valid when  $h \ll R$ .

It is thus essential that the results are not sensitive to the value of  $\xi$  used in the simulations. The switch-over point from the geometric determination to the solution of the surface thin film equations should take place at a separation distance where both methods are valid. A necessary condition for this is that the results should not be sensitive to the switch-over point in this range.

The selection of  $\xi$  is determined by considering the sensitivity of the minimum predicted thin film thickness to the selection of  $\xi$ . Therefore, to determine  $\xi$ , the value of  $h_{Crit}$  is set to zero, and the numerical solution to Cases I-IV is obtained with  $\xi = 3, 4, 5$ . Table 3 gives the numerical values of the minimum film thickness for different values of  $\xi$ . An increase in the value of  $\xi$  improves the estimate to the thin film thickness. A very small change is observed between  $\xi = 4$  and  $\xi = 5$ . It is therefore inferred that the results become independent of  $\xi$  in the region of  $4 \leq \xi \leq 5$ , and a value of  $\xi = 4$  is chosen.

$\xi$	Case I	Case II	Case III	Case IV
3	$3.363 \times 10^{-7}$	$5.619 \times 10^{-7}$	$4.716 \times 10^{-7}$	$2.078 \times 10^{-7}$
4	$1.618 \times 10^{-7}$	$3.872 \times 10^{-7}$	$2.573 \times 10^{-7}$	$1.382 \times 10^{-7}$
5	$1.649 \times 10^{-7}$	$3.296 \times 10^{-7}$	$2.146 \times 10^{-7}$	$1.094 \times 10^{-7}$

Table 3: Minimum film thickness  $h_{Min}$  (m) for Case I, Case II, Case III and Case IV

The one physical parameter present in the model is the critical film thickness  $h_{Crit}$  at which film rupture and, therefore, coalescence, occur. This is a universal parameter for a given pair of fluids, but is not known beforehand. We will therefore set this value to be consistent with the results of the four experiments. Effectively, the parameter is set to match the result of one pair of experiments, and the other pair is used as validation.

Similar to the determination of  $\xi$ ,  $h_{crit}$  is initially set to zero and the numerical results at  $\xi = 4$  are obtained for the four test cases (see 3). A global  $h_{crit}$  that is applicable to all four test cases is sought: a value such that  $1.618 \times 10^{-7} \text{m} < h_{crit} < 2.573 \times 10^{-7} \text{m}$  must be selected. The critical film thickness selected to obtain the numerical results is  $h_{crit} = 1.650 \times 10^{-7} \text{m}$ . Thus according to the solution procedure of the surface thin film model outlined in the previous section, when  $\min(h) < h_{crit} = 1.650 \times 10^{-7} \text{m}$  the volume fraction fields are merged.

The time series interface deformation plots of the droplets for selected times (for brevity) are given in figures 3–6. The results are presented at nondimensional time normalised by the droplet oscillation period  $T$ .

The interface deformation agrees qualitatively in the initial stages of the collision. At this point the surface thin film model is not applicable since the distance between the interfaces needs to be much smaller than the radius of the droplets for the model to be applicable. As the droplets continue to move closer the thin film equation becomes valid and the surface thin film model is used to calculate the film evolution.

The numerical coalescence time or rupture time has been somewhat underestimated by the model, leading to an earlier coalescence. This results in the evident delay in the dynamics after coalescence has taken place, but good qualitative agreement with the experimental results. The numerical results are obtained at a reasonable computational cost without the need to excessively refine the computational mesh.

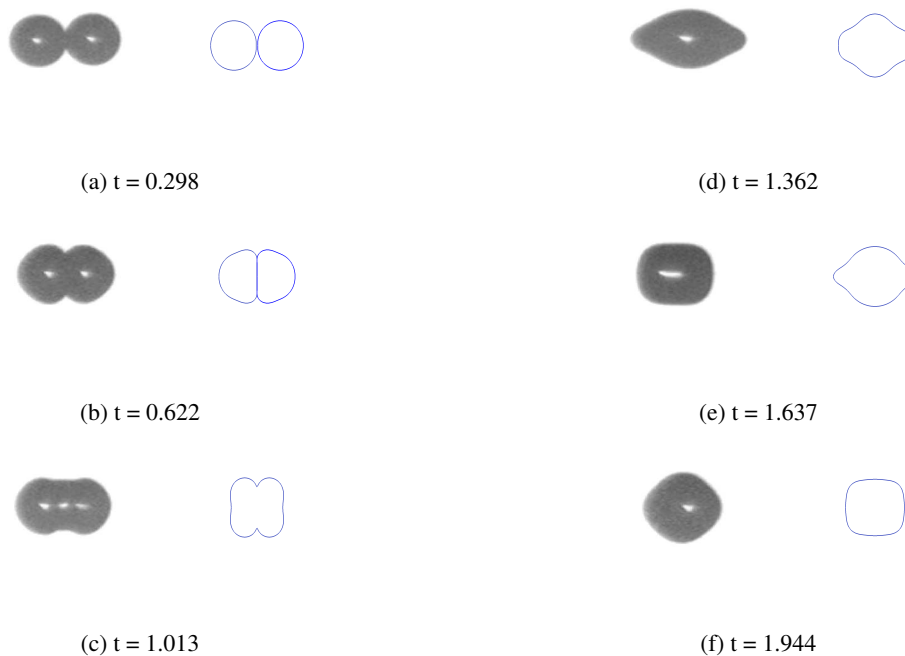


Figure 3: Time series interface shape deformations for Case I

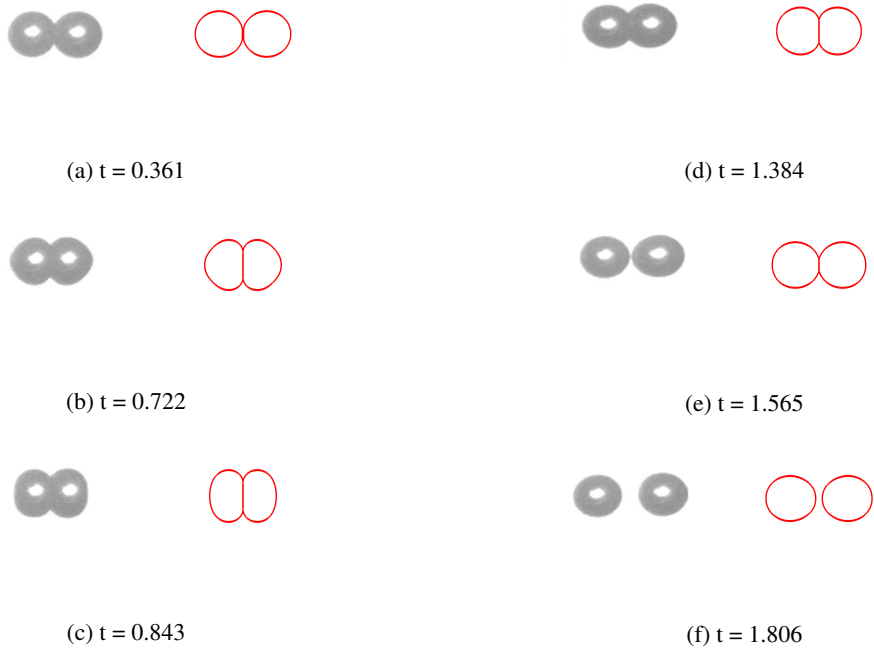


Figure 4: Time series interface shape deformations for Case II

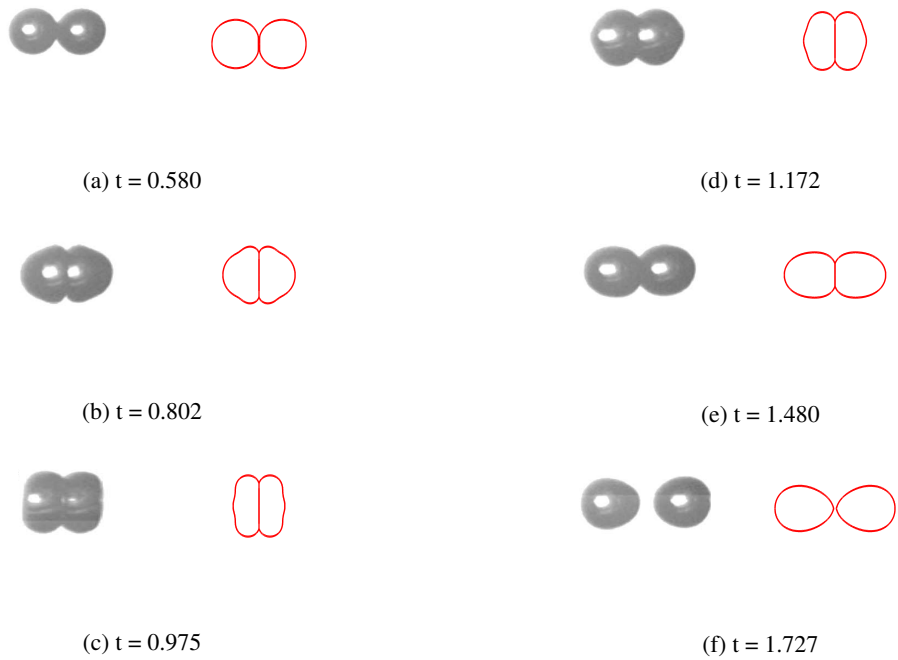


Figure 5: Time series interface shape deformations for Case III



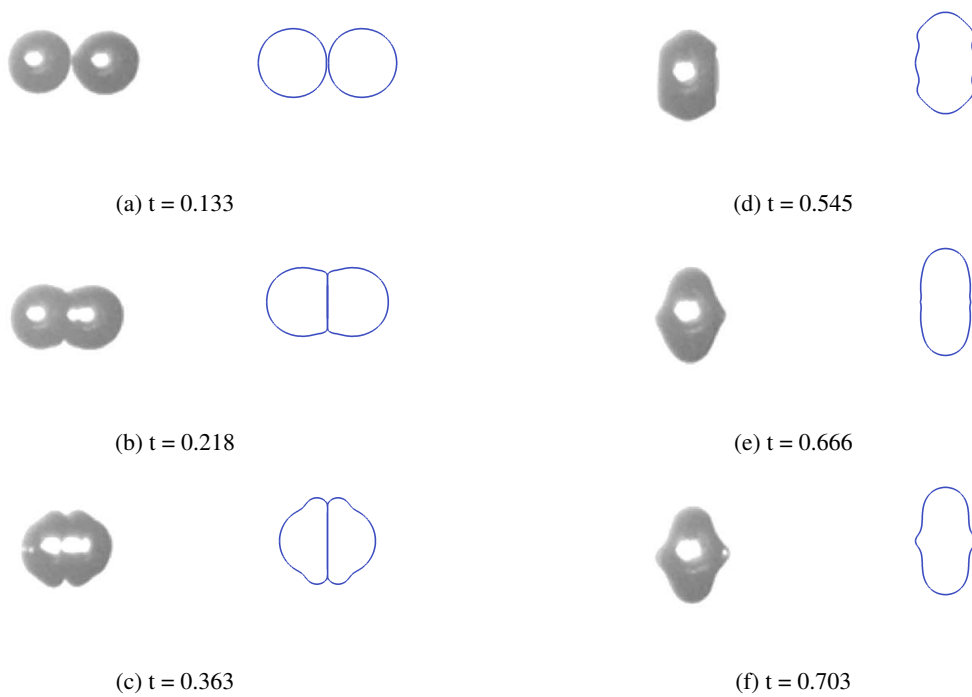


Figure 6: Time series interface shape deformations for Case IV

## CONCLUSION

To model droplet-droplet coalescence a reduced order surface thin film model coupled to a multiple marker VOF method is presented. The model is derived based on the thin film drainage theory which assumes the presence of a thin liquid film between interacting droplets. The governing set of equations are discretized using a FVM and numerical solution obtained using an implicit scheme with pressure correction.

The method is tested by simulating the binary collision of identical Tetradecane droplets in 1 atm Nitrogen and it is found to correctly predict the behaviour of the droplets before and after the duration of the collision. The numerical model slightly under predicts the instant of coalescence which results in the interface deformations after coalescence having a slight delay compared to the experimental time series.

The results of the current study demonstrated the predictive power of the surface thin film model. Although the critical film thickness was set based on the experimental data, the results agreed with all four sets of experiments of [10] under different collision conditions.

## References

- [1] C.W. Hirt and B.D. Nichols. Volume of fluid (VOF) method for the dynamics of free boundaries. *Journal of Computational Physics*, 39(1):201–225, 1981.
- [2] E. Coyajee and B.J. Boersma. Numerical simulation of drop impact on a liquid-liquid interface with a multiple marker front-capturing method. *Journal of Computational Physics*, 228(12):4444–4467, 2009.
- [3] H.A. Jakobsen, H. Lindborg, and C.A. Dorao. Modeling of bubble column reactors: Progress and limitations. *Industrial & Engineering Chemistry Research*, 44(14):5107–5151, 2005.
- [4] M.R. Nobari, Y.J. Jan, and G. Tryggvason. Head-on collision of drops—a numerical investigation. *Physics of Fluids*, 8(1):29, 1996.
- [5] J.U. Brackbill, D.B. Kothe, and C. Zemach. A continuum method for modeling surface tension. *Journal of Computational Physics*, 100(2):335–354, 1992.
- [6] J.A. Heyns and O.F. Oxtoby. Modelling surface tension dominated multiphase flows using the VOF approach. In *6th European Conference on Computational Fluid Dynamics*, 2014.
- [7] J.-D. Chen, P.S. Hahn, and J.C. Slattery. Coalescence time for a small drop or bubble at a fluid-fluid interface. *American Institute of Chemical Engineers Journal*, 30(4):622–630, 1984.
- [8] J.-D. Chen. A model of coalescence between two equal-sized spherical drops or bubbles. *Journal of Colloid and Interface Science*, 107(1):209–220, 1985.
- [9] L.R. Mason, G.W. Stevens, and D.J.E. Harvie. Multi-scale volume of fluid modelling of droplet coalescence. In *Ninth International Conference on CFD in the Minerals and Process Industries*, 2012.
- [10] K.-L. Pan, C.K. Law, and B. Zhou. Experimental and mechanistic description of merging and bouncing in head-on binary droplet collision. *Journal of Applied Physics*, 103(6), 2008.